

Analysis of a dissipative model of self-organized criticality with random neighbors

Marie-Line Chabanol and Vincent Hakim

Laboratoire de Physique Statistique†, ENS, 24 rue Lhomond, 75231 Paris Cedex 05, France.

‡associé au CNRS et aux Universités Paris VI et VII

(February 5, 2008)

We analyze a random neighbor version of the OFC stick-slip model. We find that the mean avalanche size is finite as soon as dissipation exists in the bulk but that this size grows exponentially fast when dissipation tends to zero.

PACS numbers : 05.40.+j, 05.70.Ln, 64.60.Ht

It is an appealing idea that many power laws observed in nature arise from an intrinsic trend of a large class of extended non-equilibrium systems to evolve toward critical points [1]. This concept of self-organized criticality (SOC) has therefore attracted much interest and implicit assumptions of the original model have been subjected to intense scrutiny. Several early SOC explanations assigned a crucial role to strict bulk conservation [2,3]. Non-conserving models which show SOC behavior have since been found [4,5] but in several cases the effect of a small dissipation remains unclear. An interesting model where dissipation is controlled by a parameter α , referred hereafter as the OFC model, has been introduced in [6] as a simplified version of previous modelling of fault dynamics [7]. Numerical results and supporting arguments appear to indicate that the OFC model exhibits power-law distributed avalanches in the dissipative range of α values below the conserving α_0 [6,8]. A random neighbor version of the OFC model has been studied in [9] and numerical evidence of SOC behavior has similarly been found for $\alpha_c < \alpha < \alpha_0$. Our aim here is to analyze this simpler version of the OFC model. In contrast to [9], we find that avalanches are of finite size up to the conserving limit $\alpha = \alpha_0$ but that their mean size grows exponentially fast as $\alpha \rightarrow \alpha_0$. This may explain our disagreement with [9] and can perhaps also serve as a cautionary note about similar numerical evidence obtained for local lattice models.

The model [9] consists of a set of N sites, to each of which is associated an "energy" x_i . The dynamics alternates between two phases:

- the loading phase is supposed to take place on a long time scale in the fault dynamics context. In this phase, all the x_i are below a threshold and increase continuously and simultaneously with time. This regime lasts until one energy reaches the threshold energy which we choose equal to one. At this point, an avalanche starts and the dynamics enters the avalanche phase.
- the avalanche phase is thought to be instantaneous on the time scale of the loading which can thus be neglected. The dynamics is entirely governed by energy transfers between different sites. For each $x_i \geq 1$, K different sites $j^{(i)}$ are randomly chosen. On each one, the energy is increased from $x_{j^{(i)}}$ to $x_{j^{(i)}} + \alpha x_i$ and then x_i is set to 0.

The process is repeated if some of the new energies are above one. When all the site energies are smaller than one, the avalanche ends and the system returns to the loading phase.

The parameter $0 \leq \alpha \leq 1/K$ controls the dissipation during an avalanche. If $\alpha = 1/K$, energy is conserved and the total energy of the system is constant during an avalanche. On the contrary, it decreases for $\alpha < 1/K$.

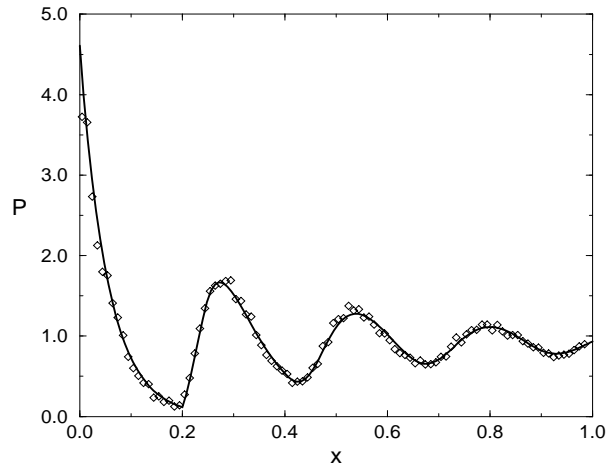


FIG. 1. Stationary distribution obtained by simulation (circles) and by solving the equations (5) and (7) (continuous line) for $K = 4$ and $\alpha = 0.2$. Simulations results are the average of $2 \cdot 10^4$ avalanches on a lattice of $N = 5 \cdot 10^3$ sites and the bin size is 0.01.

Results of simulations [9] as those reported in Fig.1, have shown that the probability distribution $P_t(x)$ of site energies tends at large times toward a non-trivial stationary distribution $P(x)$. It is, in fact, possible to obtain the exact evolution equation obeyed by $P_t(x)$ in the limit $N \rightarrow \infty$ as we now show. We define the size of an avalanche as the number of topplings during its evolution (the number of sites where the energy becomes greater or equal to the threshold). We suppose that the parameter α is small enough so that the mean avalanche size has a finite value when the system size tends to infinity. The two regimes of the dynamics contribute to the

evolution of P_t and are considered in turn. For definiteness, we fix to unity the growth rate due to the constant loading. So, in a time interval Δt between t and $t + \Delta t$, the site energies increase by $\Delta x = \Delta t$. This gives rise to M avalanches with $M = NP_t(1)\Delta x$ ($NP_t(1)$ is the density of sites which have their energy just below 1). The sites which are updated during the course of these avalanches belong to three distinct classes:

- i) the M starting sites of the avalanches the energy of which is set to zero,
- ii) the sites which through energy redistribution have their energies first increased above one and then set to zero, the total number of which we define to be $M\bar{A}_t$,
- iii) those which have their energies increased below one, the final energies of which are distributed according to a density $MB_t(x)$.

Note that we assume that the system is large enough so that the probability that a given site has been updated more than once is negligible. At $t + \Delta t$, the probability distribution of site energies has become $P_{t+\Delta t}(x)$ with

$$NP_{t+\Delta t}(x) = NP_t(x - \Delta x) - M\delta(x - 1) + MB_t(x) + M(\bar{A}_t + 1)\delta(x) - KM(\bar{A}_t + 1)P_t(x). \quad (1)$$

The last term on the r.h.s accounts for the fact that the sites of classes ii) and iii) are picked at random among the N sites and that their total number is $KM(\bar{A}_t + 1)$ (since the energy of each site above threshold is redistributed to K other sites). Taking the limit $\Delta t \rightarrow 0$, we obtain the evolution equation for $P_t(x)$, $0 \leq x \leq 1$:

$$\partial_t P_t(x) + \partial_x P_t(x) = P_t(1) [B_t(x) - K(\bar{A}_t + 1)P_t(x)] \quad (2)$$

together with the injection condition at $x = 0$,

$$P_t(0) = P_t(1) (\bar{A}_t + 1) \quad (3)$$

In order to obtain a closed equation for $P_t(x)$, it remains to determine the characteristics of the avalanches, \bar{A}_t and $B_t(x)$, in terms of $P_t(x)$. To this end, we analyze the course of an avalanche in a more detailed way. At the n -th step of an avalanche, for each site in class ii) which is set to 0, K sites are randomly chosen. Those which have their energies temporarily increased above one belong to class ii) and we denote by $a_n(x)$, $x \geq 1$, the distribution of their energies above threshold. The avalanche ends when $a_n(x) = 0$. Similarly, we call $b_n(x)$, $\alpha \leq x < 1$ the distribution of sites of class iii) produced at the n -th step. This gives therefore for $x \geq 1$,

$$a_n(x) = K \int_1^{\frac{1}{1-\alpha}} a_{n-1}(y) P(x - \alpha y) dy \quad (4)$$

For $x < 1$, one obtains an equation with the same r.h.s. but with $b_n(x)$ instead on the l.h.s.. In Eq. (4), the integral upper bound has been taken to be $1/(1 - \alpha)$ since a brief study of the series defined by $u_0 = 1$ and $u_{n+1} = 1 + \alpha u_n$ shows that $a_n(x)$ is zero if $x \geq 1/(1 - \alpha)$.

To compute the evolution of $P_t(x)$, we can restrict ourselves to consider $B_t(x)$ which is the total density $\sum_n b_n$ of sites of class iii) averaged over the M avalanches occurring between t and $t + \Delta t$. We similarly define $A_t(x)$ as the average over these avalanches of $\sum_n a_n$. From (4), $A_t(x)$ is determined from $P_t(x)$ as the solution of the linear equation for $x \geq 1$:

$$A_t(x) = K \left[\int_1^{\frac{1}{1-\alpha}} A_t(y) P_t(x - \alpha y) dy + P_t(x - \alpha) \right] \quad (5)$$

For $x < 1$, the l.h.s. is replaced by $B_t(x)$,

$$B_t(x) = K \left[\int_1^{\frac{1}{1-\alpha}} A_t(y) P_t(x - \alpha y) dy + P_t(x - \alpha) \right] \quad (6)$$

This gives B_t in terms of $A_t(x)$ and $P_t(x)$. Since $\bar{A}_t \equiv \int dx A_t(x)$, the evolution of $P_t(x)$ is determined by solving Eq. (2) together with (5) using the expression (6) for $B_t(x)$. Specializing to the steady state time independent functions, we finally obtain for $0 \leq x \leq 1$,

$$\frac{P'(x)}{KP(0)} + P(x) = \frac{\int_1^{\frac{1}{1-\alpha}} A(y) P(x - \alpha y) dy + P(x - \alpha)}{\bar{A} + 1} \quad (7)$$

where the steady state distribution $A(x)$ is determined from $P(x)$ by Eq. (5) (with the time indices dropped). At this stage, several simple remarks can be made. The size of an avalanche is the total number of sites in class ii) plus the starting site so the mean avalanche size $\bar{s} = 1 + \bar{A}$. It is useful to note that the injection condition (3) is directly obtained by integrating Eq. (7) from $x = 0$ to $x = 1$ and by using $\int_0^1 P = 1$ and $\int B = K(\bar{A} + 1) - \bar{A}$ (the last equality follows from the avalanche rule as noted above but it can also be derived by adding Eq. (5) and (6) and integrating over x). Eq. (3) gives the alternative expression of \bar{s} as $\bar{s} = P(0)/P(1)$. There are infinite avalanches with non-zero probability only if $P(0)$ is infinite or $P(1)$ is zero. Actually, we find below that both are true. Large avalanches lead to large $P(0)$ but also deplete the distribution of sites energies away from a small number of given energies with a depletion length proportional to $1/P(0)$. This leads $P(1)$ to decrease exponentially fast when $P(0)$ increases.

We now turn to the solution of Eq. (5) and (7). First, one can note that the r.h.s of Eq. (7) vanishes for $0 \leq x < \alpha$ since $B(x) = 0$ in this range. Therefore, for $x < \alpha$, one has the exact form $P(x) = P(0) \exp(-KP(0)x)$ which simply reflects the balance between the constant site creation at $x=0$ and the depletion due to site recruitment in avalanches. Besides this simple result, an analytical determination of $P(x)$ has eluded us. We have therefore solved numerically Eq. (5) and (7), taking advantage of the known form of $P(x)$ for $x < \alpha$. Given $A(x)$, this determines the r.h.s of Eq. (7) for $\alpha \leq x < 2\alpha$ and thus

$P(x)$ in this range. Continuing the process, the computation of $P(x)$ consists of solving K linear inhomogeneous differential equations. We have thus iterated the following process : solve Eq. (7) for some $P(0)$ and A , normalize P so that $\int P = 1$, set $P(0)$ to its new actual value, and use Eq. (5) to find the new A . The non-trivial satisfaction of relation (3) was used as a check of the computation. The computed $P(x)$ for $K = 4$ is shown in Fig. 1 and agrees well with simulations results. For $K = 2$, similar agreement is obtained. The computed mean avalanche size agrees with the averaged avalanche size obtained from simulations, in the range of α where they can be compared, as shown in Fig. 2 for $K = 2$. For the largest α 's, it was found necessary to use lattices of $N = 2 \cdot 10^4$ and average over $3 \cdot 10^5$ avalanches to ensure that convergence to the steady state was reached and that the results were free from finite size effects.

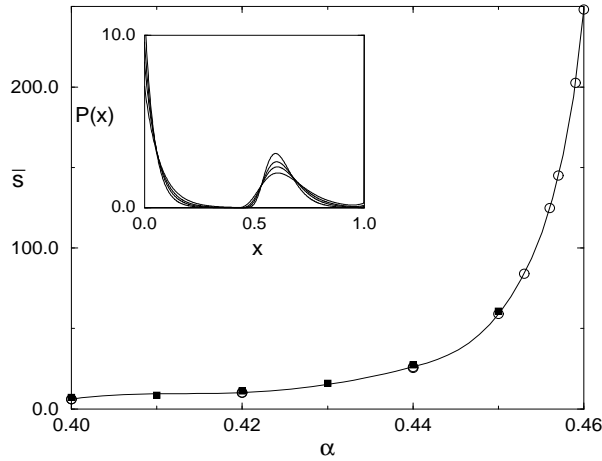


FIG. 2. Mean avalanche size *vs.* α for $K = 2$ showing solutions of (5) and (7) with $\bar{s} = \bar{A} + 1$ (circles) and results of numerical simulations (filled square). The line is a guide for the eyes. Insert : $P(x)$ obtained by solving Eq. (5, 7) for $K = 2$ and $\alpha = 0.45, 0.453, 0.456, 0.463$.

In both cases, the mean avalanche size grows very quickly when α approaches $1/K$. In ref. [9], similar results were interpreted as a divergence of the mean avalanche size at $\alpha_c = 0.2255$ for $K = 4$. With our numerical procedure, the solutions of Eq. (5) and (7) can, however, be reliably obtained up to $\alpha = 0.236$, far above the purported critical α_c . The corresponding distributions $P(x)$ are shown in Fig. 3 for $K = 4$ and do not display any singularity at $\alpha = 0.2255$. On the contrary, the four peaks of the distribution appear to sharpen smoothly as α increases. This leads us to think that they smoothly tend to δ peaks as $\alpha \rightarrow 1/4$. As shown in the insert of Fig. 2, a similar behavior is observed for $K = 2$.

The presence of sharper and sharper peaks puts a heavy demand on numerical resolution and prevents a direct numerical approach of the limit $\alpha \rightarrow 1/K$ (with our algorithm, at least). To analyze further this limit,

we focus for simplicity on the case $K = 2$. For $\alpha = 1/2$, $P(x)$ is made of two δ peaks located at $x = 0$ and $x = 1/2$ respectively while $A(x)$ is simply a δ peak at $x=1$. When α is close to $1/2$, $P(0)$ becomes large and the derivative term in Eq. (7) can balance the other terms only if $P(x)$ has a fast variation on a scale $1/P(0)$. This is indeed the case of the exact form of $P(x)$ near $x = 0$. We therefore search for A and P under the form,

$$A(x) \simeq \frac{P(0)^2}{P(1)} a[P(0)(x - 1 - 2\eta(\alpha))] \quad (8)$$

$$P(x) = P(0) \exp(-2P(0)x), \quad x \leq \alpha$$

$$P(x) \simeq \frac{1}{2} P(0) \Pi[P(0)(x - \alpha - \eta(\alpha))], \quad x \geq \alpha \quad (9)$$

where a and Π are two functions to be determined which have been normalized so that their integrals equal one and which describe the broadening for $\alpha \neq 1/2$ of the δ peaks at $x = 1$ and $x = 1/2$ respectively. The peak displacement $\eta(\alpha)$ is supposed to tend to zero as $\alpha \rightarrow 1/2$. Moreover, self-consistency requires that $P(0)\eta(\alpha) \rightarrow \infty$ when α tends toward $1/2$. This allows to neglect the weight of $B(x)/\bar{A}$ near $x = 1$ (note that $B(x)$ is the continuation of $A(x)$ for $x < 1$) as supposed in (9). Substituting the forms (8) and (9) in Eq. (5) and (7), we obtain at dominant order,

$$a(x) = \int_{-\infty}^{+\infty} \Pi(x + 2C - u/2) a(u) du \quad (10)$$

$$\Pi(x) = 4e^{-2x} \int_{-\infty}^{2x} a(u) e^u (x - u/2) du \quad (11)$$

where we have defined the constant $C = \lim_{\alpha \rightarrow 1/2} (1/2 - \alpha)P(0)$ and integrated the linear differential equation for Π . Taking Fourier transforms of (10) and (11), one obtains for $\hat{a}(\omega) = \int dx \exp(i\omega x) a(x)$, the functional equation

$$\hat{a}(\omega) = \frac{\exp(-2i\omega C)}{(1 - i\omega/2)^2} \hat{a}^2(\omega/2) \quad (12)$$

We fix the translational symmetry of Eq. (10) and (11) [$a(x) \rightarrow a(x + x_0)$, $\Pi(x) \rightarrow \Pi(x + x_0/2)$] by imposing $\int x a(x) dx = 0$. Then, the unique solution of Eq. (12) without a singularity at $\omega = 0$ is

$$\hat{a}(\omega) = \prod_{n=1}^{\infty} \frac{\exp(-2i\omega C)}{(1 - i\omega/2^n)^{2^n}} \quad (13)$$

where convergence of the infinite product enforces $C = 1/2$. One can check that the inverse Fourier transform $a(x)$ of $\hat{a}(\omega)$ is indeed a real function and is positive, as it should, since it is the convolution of the real positive functions

$$v_n(x) = \frac{2^n [2^n (x + 1)]^{2^n - 1}}{(2^n - 1)!} e^{-2^n (x + 1)} \theta(x + 1) \quad (14)$$

When $x \rightarrow -\infty$, this allows to show that $a(x)$ and $\Pi(x)$ tend extremely quickly towards zero, namely $a(2x) \sim \Pi(x) \sim \exp(-\text{cst } 4^{-x})$. Comparing the two estimations (9) of $P(x)$ near $x = \alpha$, one obtains for the peak displacement $P(0)\eta(\alpha) \simeq |\ln(1/2 - \alpha)|/\ln(4)$ as $\alpha \rightarrow 1/2$. When $x \rightarrow +\infty$, the analytic expression (13) (or directly Eq. (10) and (11)) shows that $a(x)$ and $\Pi(x)$ tend toward zero as $x \exp(-2x)$. Using this asymptotic behavior to estimate $P(1)$ gives that the mean avalanche size, $P(0)/P(1)$, diverges like $\exp(\text{cst}/(1/2 - \alpha))$ when $\alpha \rightarrow 1/2$. These predictions are compared in Fig. 4 to results obtained from the numerical solutions of Eq. (5) and (7) for $K = 2$ and different values of α . As shown in the insert, $1/P(0)$ vanishes linearly when $\alpha \rightarrow 1/2$ with a measured slope of 2.3 close to the analytical prediction of $1/C = 2$, the difference between the two being quite compatible with higher order terms in $1/2 - \alpha$. The function $a(x)$ obtained by taking the inverse Fourier transform of (13) compares well to rescaled plots of $A(y)$ with $\eta(\alpha)$ chosen so as to make the different maxima coincide [10]. Similar agreement is obtained between the analytic $\Pi(x)$ and rescaled versions of $P(y)$ around $y = 1/2$. Finally, the extremely rapid growth of the mean avalanche size when $\alpha \rightarrow 1/2$ agrees semi-quantitatively with the numerical results shown in Fig. 2 but is itself an obstacle to a precise numerical check of the predicted asymptotics. It makes it also difficult to avoid finite size effects in numerical simulations when $\alpha \rightarrow 1/K$ given that the cut-off in the avalanche size distribution scales in a mean field manner as the square of the mean avalanche size [9].

In conclusion, evidence has been presented that the random neighbor OFC model has finite avalanches as soon as the model is non-conservative with a mean avalanche size which increases extremely quickly as the conservative limit is approached. It would be interesting to assess the generality of this phenomenon and its relevance for lattice models.

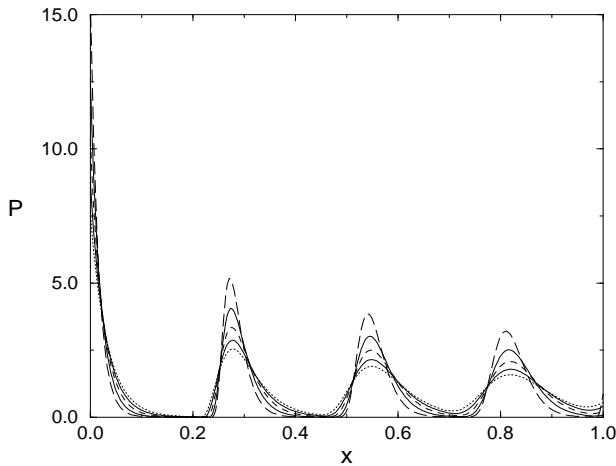


FIG. 3. Stationary distribution obtained by solving Eq. (5, 7) for $K = 4$ and $\alpha = 0.22, 0.224, 0.228, 0.232, 0.236$.

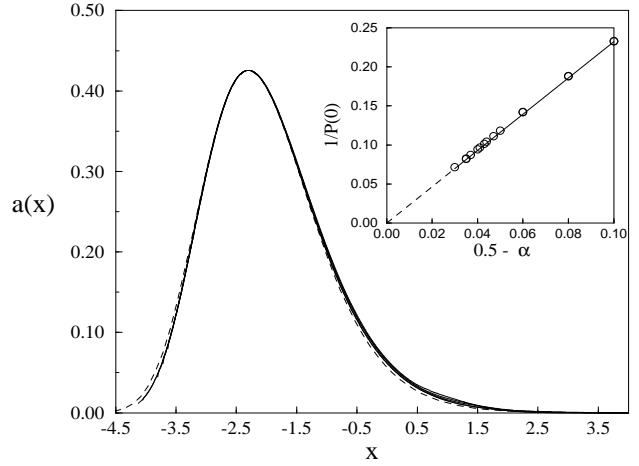


FIG. 4. $a(x)$ (dashed line) and rescaled graphs $A(y)a^*/A^*$ vs. $x = (y - 1 - 2\eta(\alpha))\rho$ (lines) for $K = 2$ and $\alpha = 0.45, 0.456$ and 0.463 . a^*/A^* is the ratio of the curve maxima and $\rho = A^*/(a^* \int A)$; $\rho/P(0) = 1.145, 1.117, 1.089$ for the graphs shown, approaching 1 as expected when $\alpha \rightarrow 1/2$. Insert: $1/P(0)$ versus $(1/2 - \alpha)$; the straight line fit has a slope of 2.3

- [1] P. Bak, C. Tang and K. Wiesenfeld, Phys. Rev. A **38**,364 (1988); G. Grinstein in *Scale invariance, interfaces and criticality* A. Mc Kane et al eds, NATO ASI Series B: Physics, Vol.344 (1995, Plenum Press, N.Y.)
- [2] T. Hwa and M. Kardar, Phys. Rev. Lett. **62**, 1813 (1989); G. Grinstein, D. H. Lee and S. Sachdev, Phys. Rev. Lett. **64**, 1927 (1990)
- [3] J. M. Carlson et al, Phys. Rev. Lett. **65**, 2547 (1990)
- [4] B. Drossel and F. Schwabl, Phys. Rev. Lett. **69**,1629 (1992); B. Drossel, S. Clar and F. Schwabl, *ibid.* **71**, 3739 (1993)
- [5] P. Bak and K. Sneppen, Phys. Rev. Lett. **71**, 4083 (1993)
- [6] Z. Olami, H.J.S. Feder and K. Christensen, Phys. Rev. Lett. **68**,1244 (1992); K. Christensen and Z. Olami Phys. Rev. A **46**,1829 (1992).
- [7] R. Burridge and L. Knopoff, Bull. Seism. Soc. Am. **57**, 341 (1967); J. M. Carlson and J. S. Langer Phys. Rev. Lett. **62**,2632 (1989)
- [8] J. E. S. Socolar, G. Grinstein and C. Jayaprakash, Phys. Rev. E **47** 2366 (1993); P. Grassberger, Phys. Rev. E **49**, 2436 (1994) A. A. Middleton and C. Tang, Phys. Rev. Lett. **74**,742 (1995)
- [9] S. Lise and H.J. Jensen, Phys. Rev. Lett. **76**, 2326 (1996).
- [10] A plot of the obtained $P(0)\eta(\alpha)$ vs. $\ln(1/2 - \alpha)$ is well fitted by a straight line of slope -0.7 close to the expected $-1/\ln(4)$. A more precise test would require solutions of Eq. (5) and (7) for values of α closer to $1/2$ than ours.